Crosstalk between YAP and TGFβ regulates *SERPINE1* expression in mesenchymal lung cancer cells

HYEON-JOON KONG[1*], EUN-JI KWON[1*], OK-SEON KWON[2], HAESEUNG LEE[3], JEONG-YUN CHOI[1], YUNG-JEONG KIM[1], WANKYU KIM[4] and HYUK-JIN CHA[1,5]

[1]College of Pharmacy, Seoul National University, Seoul 08826; [2]Stem Cell Research Center, Korea Research Institute of Bioscience and Biotechnology, Daejeon 305-806; [3]Intellectual Information Team, Future Medicine Division, Korea Institute of Oriental Medicine, Daejeon 34054; [4]Department of Life Sciences, College of Natural Science, Ewha Womans University, Seoul 03760; [5]Research Institute of Pharmaceutical Sciences, Seoul National University, Seoul 08826, Republic of Korea

Received June 2, 2020; Accepted September 29, 2020

DOI: 10.3892/ijo.2020.5153

Abstract. Serpin family E member 1 (*SERPINE1*), a serine proteinase inhibitor, serves as an important regulator of extracellular matrix remodeling. Emerging evidence suggests that *SERPINE1* has diverse roles in cancer and is associated with poor prognosis. However, the mechanism via which *SERPINE1* is induced in cancer has not been fully determined. In order to examine the molecular mechanism of *SERPINE1* expression, the present study took advantage of the isogenic pair of lung cancer cells with epithelial or mesenchymal features. Using genetic perturbation and following biochemical analysis, the present study demonstrated that *SERPINE1* expression was upregulated in mesenchymal lung cancer cells and promoted cellular invasiveness. Yes-associated protein (YAP)-dependent *SERPINE1* expression was modulated by treatment with a Rho-associated protein kinase inhibitor, Y27632. Moreover, TGFβ treatment supported YAP-dependent *SERPINE1* expression, and an enhanced TGFβ response in mesenchymal lung cancer cells promoted *SERPINE1* expression. TGFβ-mediated *SERPINE1* expression was significantly attenuated by knockdown of YAP or transcriptional co-activator with PDZ-binding motif, suggesting that crosstalk between the TGFβ and YAP pathways underlies *SERPINE1* expression in mesenchymal cancer cells.

Introduction

Despite significant advances in anticancer therapy, the recurrence, metastasis and therapeutic resistance of cancer remain serious problems leading to poor clinical outcomes (1,2). In particular, the drastic changes in cellular properties upon epithelial mesenchymal transition (EMT) are being actively studied to understand the molecular events underlying recurrence, metastasis and therapy resistance, and a number of effectors, such as zinc finger E-box binding homeobox 1 and snail family transcriptional repressor 1, mediating these molecular events have been identified and characterized (3,4).

Plasminogen activator inhibitor 1 (PAI-1), encoded by Serpin family E member 1 (*SERPINE1*), serves key roles in the regulation of extracellular matrix (ECM) remodeling by directly inhibiting plasminogen activators (PAs), such as urokinase plasminogen activator and tissue plasminogen activator (5). Considering the function of PAI-1 as the main inhibitor of PAs in ECM remodeling, which can promote the migration and invasion of cancer cells, *SERPINE1* expression in cancer has been hypothesized to inhibit these pro-metastatic effects (6). However, recent evidence has suggested that *SERPINE1* expression is associated with poor prognosis in lung cancer (7) and a high risk of metastasis in a PA-independent manner (8-11), which has been summarized in a review article (12).

While *SERPINE1* expression is induced by TGFβ stimuli, which controls PA activity (13), *SERPINE1* induction in a p53-dependent manner after TGFβ promotes replicative senescence (14). A recent study also demonstrated that TGFβ induced the formation of a complex of p53 and SMAD2/3 that enhances *SERPINE1* expression, leading to cytostatic activity (15). In addition, 'non-SMAD pathways' such as p53, c-SRC, EGFR and MAPK are involved in TGFβ-dependent *SERPINE1* expression in the context of vascular disorders (16) and pulmonary fibrosis (17). These reports suggest that other signaling pathways may contribute to TGFβ-stimulated *SERPINE1* expression in a context-dependent manner.

The Hippo pathway, in which loss-of-function mutations activate yes-associated protein (YAP) and transcriptional co-activator with PDZ-binding motif (TAZ) and lead to robust cell proliferation and survival, has been strongly implicated in several cancer-associated processes, such as tumorigenesis (18), EMT (19,20), metastasis (21) and therapy resistance (22). Thus,

Correspondence to: Professor Hyuk-Jin Cha, Research Institute of Pharmaceutical Sciences, Seoul National University, 1 Gwanak-ro, Gwanak-gu, Seoul 08826, Republic of Korea
E-mail: hjcha93@snu.ac.kr

*Contributed equally

Key words: serpin family E member 1, plasminogen activator inhibitor 1, TGFβ, yes-associated protein, epithelial mesenchymal transition, invasion, crosstalk

the Hippo pathway has been extensively studied in an effort to identify molecular targets to inhibit YAP/TAZ-dependent gene responses. Several small molecules have been reported to inhibit YAP/TAZ activity, including Y-27632 as an inhibitor of Rho-associated protein kinase (ROCK) (23,24). In addition, YAP or TAZ can interact with the SMAD2/3-4 complex and facilitate SMAD nuclear translocation (25,26) to control SMAD-dependent gene responses. Crosstalk between YAP/TAZ and the canonical TGFβ pathway has also been observed, as the absence of YAP attenuates TGFβ-induced profibrotic gene responses (27).

Using the lung cancer cell lines that demonstrate clear cellular properties of EMT, the present study aimed to examine the molecular mechanism of *SERPINE1* induction in cancer cells.

Materials and methods

Establishment of cell lines and cell culture. The mesenchymal-like lung cancer cells (Transdifferentiated cell; TD) were established by chronic exposure of TGFβ to a A549 lung cancer cell line (purchased from Korean Cell Line Bank; cat. no. 10185) as described previously (28). To maintain TD cells, cells were treated with Hyclone DMEM/High glucose (Cytiva; cat. no. SH30243.01), 10% FBS (cat. no. EF:35-015-CV; Corning, Inc.) and Gentamicin (0.1%; cat. no. 15780-060; Gibco; Thermo Fisher Scientific, Inc.) at 37˚C with 5% CO_2, along with a low dose of TGFβ (2 ng/ml; cat. no. cyt-716; Prospec-Tany TechnoGene) every 3 days at 37˚C.

For generation of TD cell lines harboring *SERPINE1* knockdown via short hairpin (sh)RNA (cat. no. SHCLNG-NM_000602; Sigma-Aldrich; Merck KGaA), pLKO.1-shControl (cat. no. SHC016; Sigma-Aldrich; Merck KGaA) and sh*SERPINE1* vector were introduced using a lentivirus. The infected cells were selected with puromycin. In order to examine TGFβ response, a 16 h starvation with TGFβ prior to the experiment in TD cells was performed. All genetic perturbations (e.g. knockdown or transient transfection) were performed without TGFβ treatment.

For cell density dependent experiment, A549 or TD cells were grown at the indicated cell density (magnification, x100; scale bar, 80 μm). A cell number of 100% confluence equalled ~3.0x10^6 cells. Indicative cell density was obtained by a serial dilution with normal culture media.

Reagents and antibodies. TGFβ recombinant protein (cat. no. CYT-716) was purchased from ProSpec-Tany TechnoGene Ltd., and Y27632 (cat. no. 1293823) was obtained from BioGems Ltd. Cells were treated with 10 μM Y27632 for 24 h at 37˚C. Small interfering (si)RNA targeting *SERPINE1*, SMAD4, YAP1 and TAZ were obtained from Bioneer Corporation. Antibodies against E-cadherin (cat. no. 4065) was purchased from Cell Signaling Technology, Inc. *SERPINE1* (cat. no. ab125687) and β-actin (cat. no. sc-47778) were obtained from Abcam and Santa Cruz Biotechnology, Inc., respectively.

Total RNA extraction via reverse transcription-quantitative PCR (RT-qPCR). Total cellular RNA was extracted using TRIzol® (cat. no. 17061; Invitrogen; Thermo Fisher Scientific, Inc.), followed by RT-PCR to generate the first strand cDNA using RT Master mix (cat. no. RR036A; Takara Bio, Inc.). The RT conditions were as follows: 37˚C for 15 min, 85˚C for 5 sec and held at 4˚C. The synthesized cDNA was subjected to qPCR using TB green premix Ex Taq (Takara Bio, Inc.; cat. no. RR420), PrimeScript™ 1st strand cDNA Synthesis kit (Invitrogen; Thermo Fisher Scientific, Inc.) and SYBR-Green-based Real-time PCR (Takara Bio, Inc.) using Roche Light Cycler 480 II (Roche Diagnostics, Inc.) following the manufacturer's instructions. The data analysis was performed as described previously, using the $2^{-\Delta\Delta Cq}$ method (29). Primer sequences are presented in Table I.

Immunoblotting. Cell were lysed with RIPA buffer with 10 μM sodium vanadate and 1 mM protease inhibitor (Roche Diagnostics, Inc.) followed by immunoblotting as described previously (30). Protein determination prior to protein loading was performed with a BCA assay. The samples were loaded to 7.5 or 10% SDS-PAGE gels and were blotted to a PVDF membrane (Immobilon®-P; cat. no. IPVH00010; Merck KGaA). The blotted membrane was incubated with skim milk [1 mg in TBS-Tween (25%); 20 ml; cat. no. 232100; BD Difco; Becton-Dickinson and Company] for 1 h at room temperature. Primary antibodies (all 1:1,000) for PAI-1 (cat. no. ab125687; Abcam), E-cadherin (cat. no. 3195S; Cell Signaling Technology, Inc.), phosphorylated (p)-YAP (cat. no. 4911S; Cell Signaling Technology, Inc.), YAP (cat. no. SC-101193; Santa Cruz Biotechnology, Inc.) and β-actin (cat. no. SC-47778; Santa Cruz Biotechnology, Inc.) were incubated for overnight at 4˚C. After washing three time with TBS-Tween solution, the mouse or rabbit secondary antibodies [Peroxidase AffiniPure Goat Anti-Mouse IgG (H+L); cat. no. 115-035-003; Jackson ImmuniResearch Laboratories, Inc.; and Peroxidase AffiniPure Goat Anti-Rabbit IgG (H+L); cat. no. 111-035-003; Jackson ImmuniResearch Laboratories, Inc.] were incubated for 1 h at room temerature. The visualization was peformed with ECL blotting kit (cat. no. 16026; West-Queen; iNtRON Biotechnology).

Transfection and dual-luciferase assay. Transfections were performed using Lipofectamine® 2000 (Invitrogen; Thermo Fisher Scientific, Inc.) in accordance with the manufacturer's instructions. siRNA for SERPINE1 (Thermo Fisher Scientific, Inc.; cat. no. AM16708) and control siRNA (Thermo Fisher Scientific, Inc.; cat. no. AM4611) transfection was performed using DharmaFECT (cat. no. T-2001-03; GE Healthcare Dharmacon, Inc.) according to the manufacturer's instruction.

shSERPINE1 #2: 5'-CCGGTTTAGTGTTAATGACTCTT TCCTCGAGGAAAGAGTCATTAACACTAAATTTTTG-3'; shSERPINE1 #4: 5'-CCGGAGACCAACAAGTTCAACTAT ACTCGAGTATAGTTGAACTTGTTGGTCTTTTTTG-3'.

For the luciferase assay for SMAD4 activity, 8X GTIIC luciferase reporter vector (kindly gifted by Professor Mo Jung-Soon at Ajou University), as well as pRL *Renilla* luciferase control reporter vector (cat. no. E223A; Promega Corporation), were transfected into cells. A reporter assay was conducted according to the Dual-Luciferase Reporter assay system (Promega Corporation) using Lipofectamine 2000 (Invitrogen; Thermo Fisher Scientific, Inc.; cat. no. 52887). After 24 h transfection, reporter activity was performed with the reporter assay kit (Promega Corporation) as described previously (31). The luciferase activity was normalized to *Renilla* luciferase

Table I. Primer sequences for reverse transcription-quantitative PCR.

Gene	Primer sequence (5'→3')
GAPDH	F: GCATCCTGCACCACCAACTG
	R: GCCTGCTTCACCACCTTC TT
CDH1	F: TGCCCAGAAAATGAAAAACG
	R: GTGTATGTGGCAATGCGTTC
CDH2	F: GACAATGCCCCTCAAGTGTT
	R: CCATTAAGCCGAGTGATGGT
CTGF	F: CCAATGACAACGCCTCCTG
	R: TGGTGCAGCCAGAAAGCTC
SERPINE1	F: TTGAATCCCATAGCTGCTTGAAT
	R: ACCGCAACGTGGTTTTCTCA
YAP	F: GTGAGCCTGTTTGGATGATG
	R: CACTGGACAAAGGAAGCTGA

F, forward; R, reverse; CDH, cadherin; YAP, yes-associated protein; *SERPINE1*, serpin family E member 1.

activity. For YAP reporter activity, 8X GTIIC (for recognition of TEAD binding domain; cat. no. 34615; Addgene) was transfected to cells after incubation with Lipofectamine® 2000 (cat. no. 52887; Invitrogen; Thermo Fisher Scientific, Inc.) for 20 min according to the manufacturer's instructions.

Migration and Transwell invasion assay. For wound healing assay, after 24 h of incubation under serum starvation (0.1% FBS) conditions, the TD cell layer was scratched using a sterile micropipette tip. Cell migration was monitored with the light microscope (magnification, x40; Olympus Corporation) and live images were captured using a JuLi stage real-time imaging system (NanoEntek, Inc.) over 48 h.

For Transwell invasion assay, Transwells were embedded with Matrigel. In brief, Transwells (6.5 mm) with 8-μm pore polycarbonate membrane insert (cat. no. 3422; Corning, Inc.) were embedded with Matrigel for 2 h at 37˚C (BD Bioscience) and the bottom of the Matrigel-embedded insert was coated with 0.2% gelatin. Cells were cultured under normal culture medium Hyclone DMEM/High glucose (Cytiva, cat. no. SH30243.01), 10% FBS (cat. no. EF:35-015-CV; Corning, Inc.) and Gentamicin (0.1%; cat. no. 15780-060; Gibco; Thermo Fisher Scientific, Inc.) at 37˚C with 5% CO_2. At 24 h after $2x10^5$ cells were loaded in the Transwell assay, the Transwell membrane was fixed with 4% formaldehyde for 10 min at room temperature and stained with 0.1% violet at room temperature (25˚C). Images of the Transwell membrane were captured using light microscopy (magnification, x40) The area of invaded cells was measured using ImageJ software (National Institutes of Health; version 1.52v).

Tumor spheroid invasion assay. The 3D tumor spheroid invasion assay was performed as previously described (32). In brief, spontaneously formed spheroids derived from TD cells were implanted into self-assembling collagen I gels (Vitrogen; Cohesion Technologies) supplemented with minimal essential media and 2% FBS and were cultured for 7 days under standard cell culture conditions.

Zymography. Conditioned media (Hyclone DMEM/High glucose; cat. no. SH30243.01) with 10% FBS (cat. no. 35-15-CV; Corning, Inc.) and 0.1% gentamycin (REF:15780-060; Gibco; Thermo Fisher Scientific, Inc.) from cells maintained at 37˚C, 5% CO_2 were concentrated using centricon (EMD Millipore; 30 kDa cut). Zymography analysis using Coomassie blue R250 staining (25˚C, 15 min) after loading to 8% gelatin B gel, was performed as described previously (33).

Cancer cell line transcriptome data analysis. As described previously (34) RNA sequencing (RNA-seq) data of 932 cancer cell lines were obtained from the NCI's Genomic Data Commons (https://gdc.cancer.gov/) in the BAM file format. Gene-level read count and Transcripts per Million (TPM) were quantified using RSEM v.1.3.1. (https://deweylab.github.io/RSEM/) with Gencode v19 annotation(https://www.gencodegenes.org/human/release_19). A total of 18,965 genes annotated as 'protein-coding gene' were used for subsequent analysis. The EMT score for each cell line was defined as the Kolmogorov-Smirnov (K-S) statistic, which measures the differences in the distribution of gene expression levels (TPM) of EMT genes compared with those of the rest of the genes. EMT genes were obtained from the MSigDB: 'hallmark epithelial mesenchymal transition' (https://www.gsea-msigdb.org/gsea/msigdb). The K-S statistic of each cell line was calculated using ks.test function in R software(version 3.6.3). To compare the expression patterns of mesenchymal-like and epithelial-like cell lines, the EMT^+ and EMT^- cell groups were selected as the top 10% and bottom 10% cell lines, respectively, based on the EMT score. Gene-level read counts of A549 and TD cells were downloaded from the Gene Expression Omnibus (GSE135402). The differences in gene expression between TD cells and A549 cells or between EMT^+ and EMT^- cell groups were calculated using the DESeq2 package (35) (version 1.28.1) in R (version 3.6.3).

The Cancer Genome Atlas (TCGA) data processing and analysis. RNA-seq and clinical data of patients with lung adenocarcinoma (LUAD) in the TCGA study were obtained from the Broad GDAC firehose (https://gdac.broadinstitute.org/; data version 2016_01_28). A total of 494 patients with ≥1 month of follow-up clinical record information were used for survival analysis (women, 263; men, 231; median age, 66). Patients were divided into two groups according to the median value (TPM) of *SERPINE1* gene expression. Upper (n=247) and lower (n=247) groups were defined as 'high' and 'low' groups. In similar, CTGF high (n-247) and low (n=247) groups were defined. Overall survival and recurrence-free survival analysis were performed to test the difference in the survival rate between the groups using the survival package (https://cran.r-project.org/package=survival; version 3.2-7) in R (version 3.6.3). The hazard ratio and P-value were computed using Cox proportional hazards regression analysis and the log-rank test, respectively.

Pathway enrichment analysis. RNAseq data of A549 and TD (GSE135402) was used. Among the 3,675 differentially

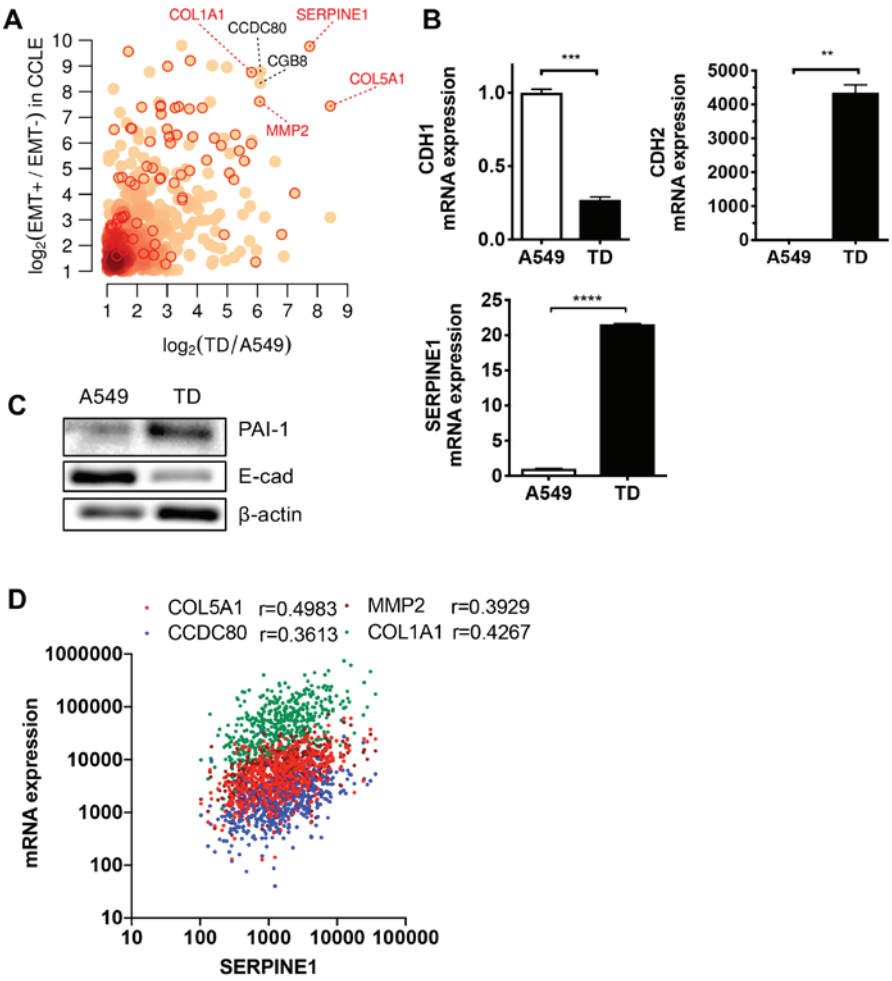

Figure 1. High *SERPINE1* expression in mesenchymal lung cancer cells. (A) Differentially upregulated genes in both the EMT^{+} vs. EMT^{-} cell groups of the CCLE dataset and in TD vs. A549 cell groups. Red circles indicate known EMT genes annotated by MSigDB (http://software.broadinstitute.org/gsea/msigdb). (B) Relative mRNA expression levels of *CDH1*, *CDH2* and *SERPINE1* in A549 and TD cells. (C) Immunoblotting for PAI-1 and E-cad in A549 and TD cells. β-actin was used as an equal protein loading control. (D) Correlation of *SERPINE1* mRNA expression with indicated genes in patients with lung adenocarcinoma. **P<0.01, ***P<0.001, ****P<0.0001. E-cad, E-cadherin; *SERPINE1*, serpin family E member 1; COL1A1, collagen type Iα1 chain; EMT, epithelial mesenchymal transition; CCLE, Cancer Cell Line Encyclopedia; *CDH*, cadherin; PAI-1, Plasminogen activator inhibitor 1.

expressing genes (DEG) identified between A549 and TD, 111 SMAD4 downstream genes were identified using web-based tool 'EnrichR'(https://maayanlab.cloud/Enrichr/). Pathway enrichment analysis was performed based on the geneset of public annotation in Gene Ontology (GO) via EnrichR.

Statistical analysis. Data are presented as the mean ± SD Statistical significance between two groups was determined using t-test analysis (unpaired). Statistical significance among the three groups and between groups was determined using One-way ANOVA following the Tukey's multiple comparison test (GraphPad Prism 7.0; GraphPad Software, Inc.). P<0.05 was considered to indicate a statistically significant difference. Number of experimental repeats was >3.

Results

High SERPINE1 expression in mesenchymal lung cancer cells. Our previous studies established isogenic mesenchymal lung cancer cells [A549 transdifferentiated cells (A549TD), hereafter TD] derived from A549 cells subjected to long-term exposure to TGFβ (similar to a previously described method) (36), with typical EMT features such as chemoresistance and prometastatic activity (28,37-39). To identify key genes responsible for the mesenchymal cell state, the current study examined genome-wide mRNA expression profiles from A549 and TD cells, along with a panel of human cancer cell lines (CCLE) (40). The most upregulated gene in cells with enriched mesenchymal properties was *SERPINE1*, followed by other known EMT markers such as collagen type Iα1 chain (*COL1A1*), Coiled-Coil Domain Containing 80, *MMP2* and *COL5A1* (Fig. 1A). As predicted, *SERPINE1* expression was significantly increased in TD cells, in parallel with lower levels of cadherin 1 (*CDH1*; encoding E-cadherin) and higher *CDH2* (encoding N-cadherin) compared with parental A549 cells (Fig. 1B). The protein level of PAI-1 (encoded by *SERPINE1*) was higher in TD cells compared with A549 cells (Fig. 1C). Consistently, four genes (*COL1A1*, *CDC80*, *MMP2* and *COL5A1*) were found to be closely associated with *SERPINE1* expression in 494 patients with lung adenocarcinoma (TCGA) (Fig. 1D).

SERPINE1 contributes to cancer cell invasive properties. Despite the well-known physiological role of *SERPINE1*

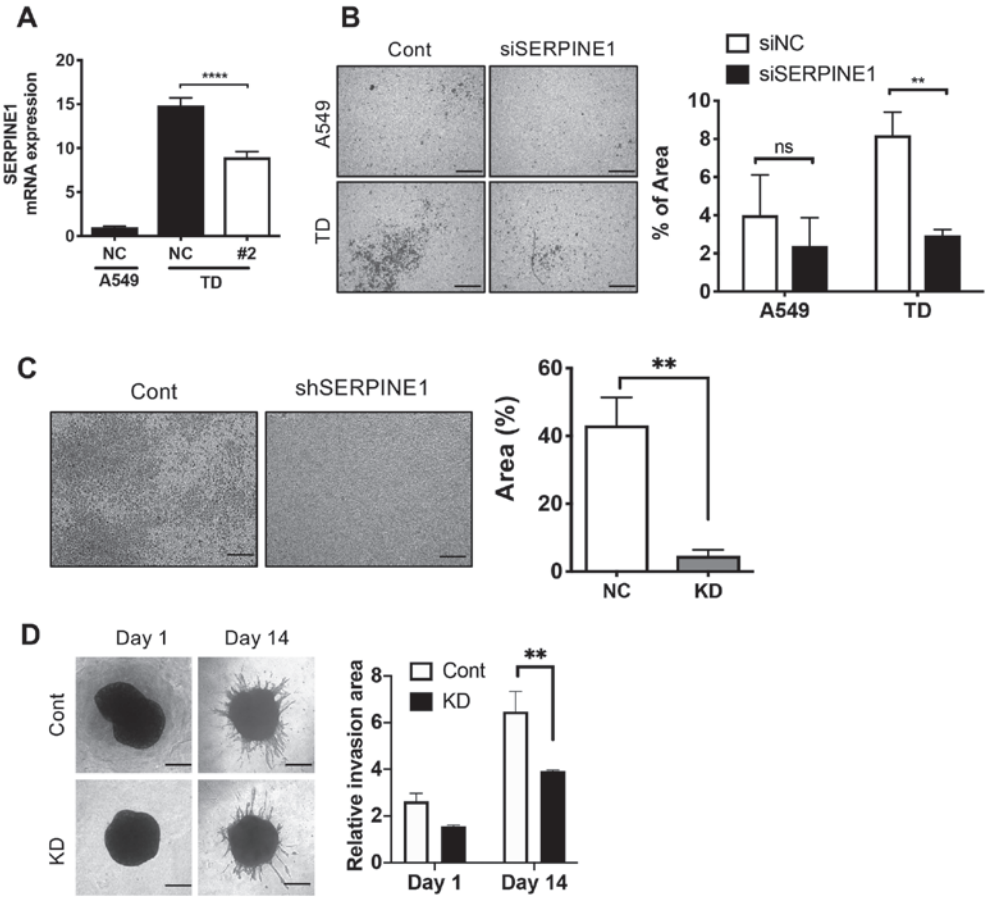

Figure 2. *SERPINE1* contributes to cancer cell invasive properties. (A) mRNA expression of *SERPINE1* in A549 and TD cells after knockdown with *SERPINE1* shRNA. Representative microscopic images (left) of invaded cell numbers in a two-chamber invasion model after knockdown either with (B) *SERPINE1* siRNA or (C) shRNA, relative invasion area was graphically presented (right). Magnification, x40; scale bar, 200 μm. (D) Microscope images of tumor spheroid of control TD cells (left), and graphical presentation of invasive area (right). Magnification, x100; scale bar, 80 μm. **P<0.01, ****P<0.0001. si, small interfering RNA; *SERPINE1*, serpin family E member 1; NC, negative control; Cont, control; shRNA, short hairpin RNA; KD, knockdown.

in inhibiting PAs, *SERPINE1* induction promotes invasion and migration in diverse cancer types in a PA-independent manner (11). To examine whether the elevated expression of *SERPINE1* in TD cells (Fig. 1B and C) accounted for the high invasiveness of TD cells (28,37), *SERPINE1* expression was knockdown using siRNA in TD cells (Fig. 2A), and a cell invasion assay was performed. Consistent with previous reports (9,41,42), the highly invasive properties of TD cells (28,37) were significantly attenuated by knockdown of *SERPINE1*, while knockdown in A549 cells had no significant effect on cell invasion (Fig. 2B). Stable knockdown of *SERPINE1* with shRNA was achieved; the clone#2 demonstrated the most significant knockdown efficiency (Fig. S1A) and was selected for further study. Consistent with the results of siRNA, stable knockdown of *SERPINE1* using shRNA had an inhibitory effect on cell invasion (Fig. 2C). The attenuated invasiveness by loss of *SERPINE1* expression was further validated via tumor spheroid invasion assay (Fig. 2D) (32).

However, inconsistent with the findings of a previous report (43), *SERPINE1* knockdown in TD cells with shRNA (Fig. S1A) only had marginal effects on cellular migration (Fig. S1B). Moreover, transient knockdown of SERPINE1 with siRNA (Fig. S1C) had a negligible effect on the high activity of MMP9 in TD cells (Fig. S1D).

YAP-dependent SERPINE1 expression. Previous work has revealed that *SERPINE1* is induced by ectopic expression of TAZ, along with connective tissue growth factor (CTGF), a well-established YAP/TAZ downstream target gene (44), which is frequently used as a marker to determine endogenous YAP-TEAD activity in a number of study (44,45). The present study identified that ectopic expression of either wild-type YAP or a constitutively active mutant lacking inhibitory phosphorylation of YAP was sufficient to induce *SERPINE1* expression in both A549 and TD cells (Fig. 3A). It is important to note that despite a comparable level of YAP expression in A549 and TD (data not shown), the nuclear level of YAP appeared to be significantly higher in TD cells compared with A549 cells, regardless of cell density (Fig. S2A). This observation was consistent with the higher mRNA expression level of *SERPINE1* in TD cells compared with A549 cells (Fig. 3A).

To confirm the involvement of the Hippo-YAP pathway in *SERPINE1* expression, Hippo signaling was re-activated by Y27632, a ROCK inhibitor (46) that markedly decreases YAP reporter activity (e.g. 8X GTIIC reporter activity) (Fig. 3B). Protein expression levels of YAP, TAZ and p-YAP at serine 127 were not different between A549 and TD cells (Fig. S2B). Treatment with Y27632 was sufficient to attenuate *SERPINE1* expression (Fig. 3C) in a time- (Fig. 3D) and dose- (Fig. 3E and F) dependent manner, along with a reduction

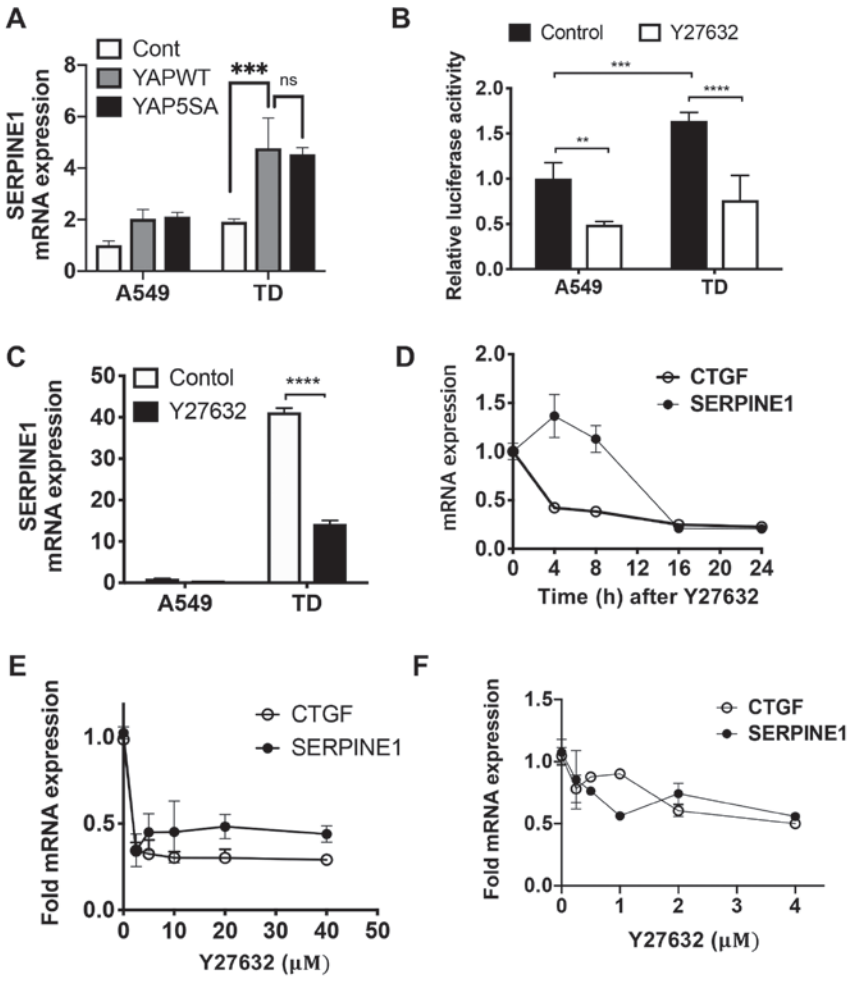

Figure 3. YAP-dependent *SERPINE1* expression. (A) Relative mRNA expression of *SERPINE1* after Flag-mock, Flag-YAP and Flag-YAP5SA were transfected in A549 and TD cells. (B) GTIIC luciferase activity in A549 and TD cells at 24 h after Y27632 (10 μM) treatment. (C) mRNA expression of *SERPINE1* expression in A549 and TD cells at 24 h after Y27632 (10 μM) treatment. (D) Relative mRNA expression levels of CTGF and *SERPINE1* after Y27632 (10 μM) treatment at indicative timepoint. (Relative mRNA expression of CTGF and *SERPINE1* at 24 h after (E) high concentration (10- 40 μM) and (F) low concentration (0.25-4 μM) of Y27632 treatment. **P<0.01, ***P<0.001, ****P<0.0001. *SERPINE1*, serpin family E member 1; WT, wild-type; YAP, yes-associated protein; ns, not significant; CTGF, connective tissue growth factor; YAP5SA, constitutively active mutant lacking inhibitory phosphorylation of YAP.

in CTGF. As Y27632 treatment had no effect on either *CDH1* or *CDH2*, the repression of *SERPINE1* by Y27632 may not be mediated by a loss of mesenchymal properties in the TD cells (Fig. S2C).

Involvement of the TGFβ-SMAD4 axis in YAP-dependent SERPINE1 expression. It has been well established that TGFβ serves as a key stimuli for *SERPINE1* expression in diverse cell line models (13). In addition, crosstalk with 'non-SMAD pathways' is involved in TGFβ-dependent *SERPINE1* expression (15,16,47). Although TGFβ treatment alone upregulated *SERPINE1* expression in both cells, TGFβ-mediated *SERPINE1* expression was induced to a greater degree in TD cells compared with A549 in a dose- (Fig. 4A) and time-dependent manner (Fig. 4B). Increased expression of PAI-1 protein by TGFβ also occurred, while knockdown of *SERPINE1* using siRNA markedly lowered PAI-1 protein expression (Fig. 4C).

Smad-binding element reporter activity, which is used to determine SMAD2/3 dependent gene responses (48), was markedly enhanced in TD cells (Fig. 4D). These data suggested that *SERPINE1* induction may be facilitated by the enhancement of TGFβ-dependent gene responses. Given that *SERPINE1* expression was regulated by both YAP and TGFβ, it was conclude that the YAP pathway and SMAD4-dependent TGFβ signaling interact upon TGFβ stimulation. To evaluate the hypothesis of a crosstalk between TGFβ signaling and YAP, pathway enrichment analysis of 111 genes, which are regulated by the SMAD4 transcription factor in the DEGs in A549 and TD cells, was performed. The second most enriched pathway was the Hippo pathway ($P=1.4x10^{-4}$) after TGFβ signaling ($P=0.2x10^{4}$) (Fig. 4E). As predicted, *CTGF* expression, indicating a YAP-dependent gene response, was rapidly enhanced upon TGFβ treatment in TD cells (Fig. 4F), similar to SRE reporter activity (Fig. 4D). Of interest, knockdown of SMAD4 in TD cells failed to affect basal levels of *SERPINE1* expression, whereas TGFβ-mediated *SERPINE1* expression was attenuated by SMAD4 knockdown (Fig. 4G). Moreover, TGFβ-mediated *SERPINE1* expression was significantly decreased by knockdown of YAP (Fig. 4H). This effect was more pronounced when YAP and TAZ were simultaneously depleted (Fig. 4I), suggesting that YAP and TAZ may be required for TGFβ-SMAD4-dependent *SERPINE1* expression in mesenchymal lung cancer cells. The knockdown efficiencies of siRNAs of SMAD4, YAP and TAZ with or without treatment

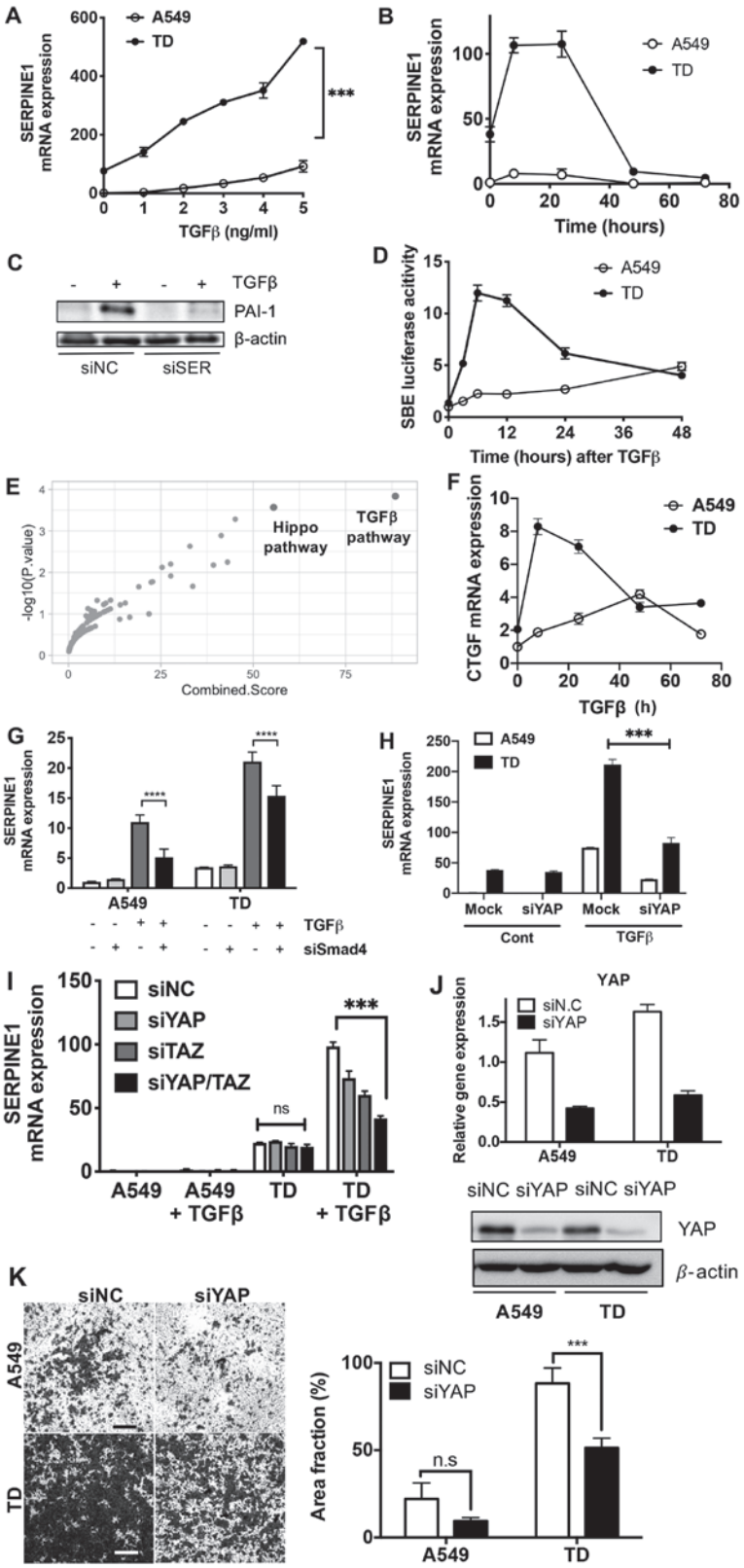

Figure 4. Involvement of the TGFβ-SMAD4 axis in YAP-dependent *SERPINE1* expression. (A) *SERPINE1* mRNA expression in A549 and TD cells at 24 h after TGFβ treatment with the indicated concentrations. (B) Relative mRNA expression of *SERPINE1* in A549 and TD cells at indicative time-point after TGFβ (2 ng/ml) treatment. (C) Immunoblotting analysis for PAI-1 protein expression at 24 h after TGFβ (2 ng/ml) treatment with siNC or siSER. (D) SBE luciferase activity in A549 and TD cell lines at indicated time-points after TGFβ (2 ng/ml) treatment. (E) Enriched pathway in the 111 genes regulated by SMAD4 in DEG of A549 and TD cells. Highlighted red dots indicate the TGFβ and Hippo pathways. (F) mRNA expression of CTGF in A549 and TD cells at indicated time-point after TGFβ treatment (2 ng/ml). mRNA expression of *SERPINE1* in A549 and TD cells at 24 h after TGFβ (2 ng/ml) treatment after knockdown of (G) SMAD4, (H) YAP and (I) YAP/TAZ with siRNA transfection. (J) mRNA expression (top) and protein (bottom) of YAP after knockdown of YAP, β-actin was used for protein loading control. (K) Representative images (magnification, x40) of invaded cells from a two-chamber invasion model after knockdown with YAP siRNA (left), graphical representation of area fraction of invaded area (right). ***P<0.001, ****P<0.0001. siSER, small interfering RNA serpin family E member 1; NC, negative control; *SERPINE1*, serpin family E member 1; YAP, yes-associated protein; TAZ, transcriptional co-activator with PDZ-binding motif; CTGF, connective tissue growth factor; PAI-1, plasminogen activator inhibitor 1; SBE, Smad-binding element; ns, not significant.

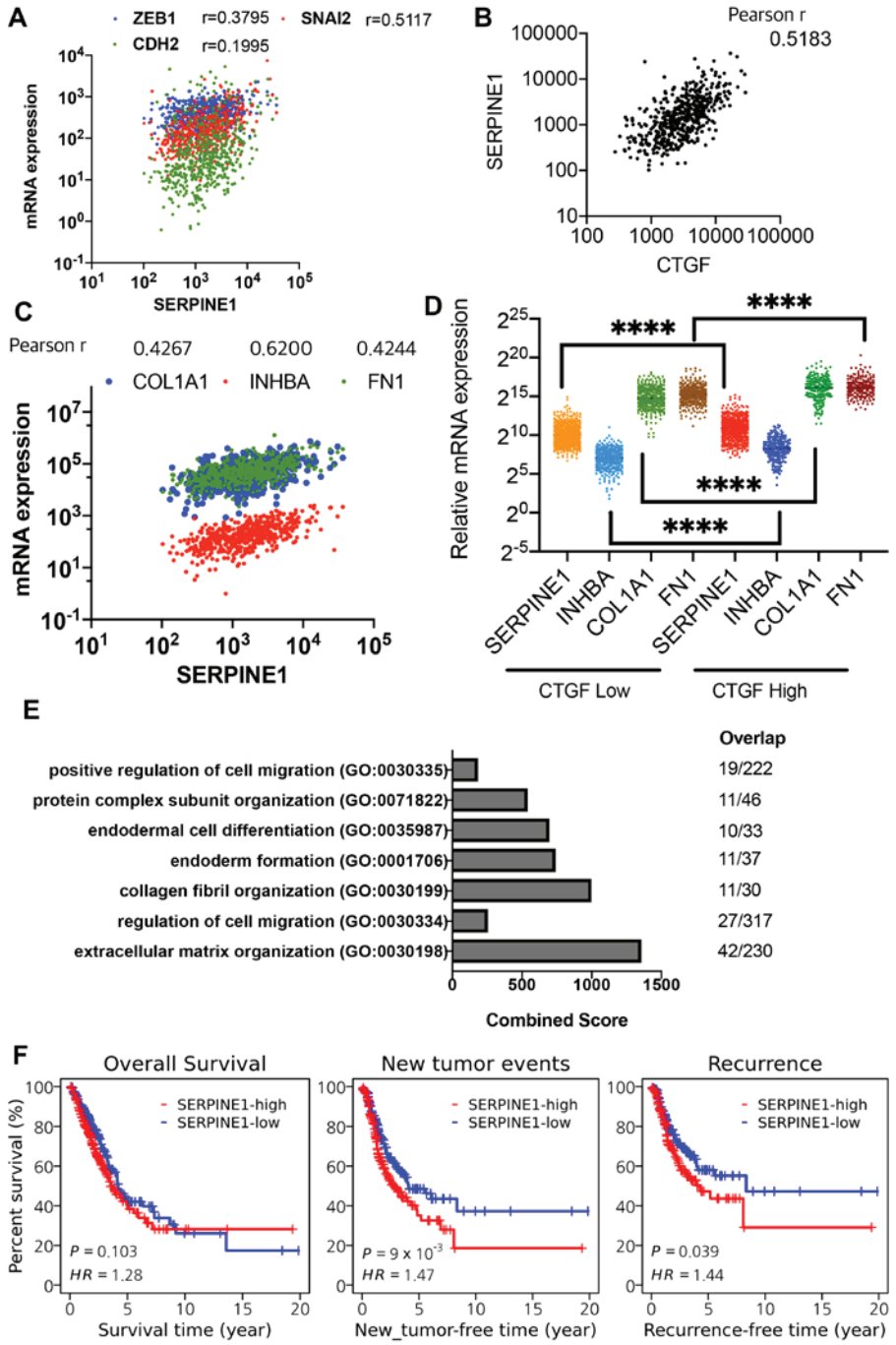

Figure 5. Regulation of *SEPINE1* expression in the patients with LUAD. Correlation of mRNA expression of *SERPINE1* with (A) epithelial mesenchymal transition marker genes, (B) CTGF and (C) SMAD4 downstream genes in patients with LUAD. (D) Comparison between the high- and low-expression group for CTGF of average expression levels from 566 patients with lung cancer from TCGA cohort, in terms of relative mRNA expression of indicated genes in patients with LUAD. (E) GO analysis with genes highly correlated with *SERPINE1* in patients with LUAD. Combined score of each GO is presented as a bar graph (left) and number of genes overlapped in each GO is illustrated (right). (F) Comparison between the high- and low-expression groups for *SERPINE1* in terms of overall survival, new tumor event-free survival and locoregional recurrence-free survival in patients with LUAD. ****P<0.0001. GO, Gene Ontology; *SERPINE1*, serpin family E member 1; HR, hazard ratio; CTGF, connective tissue growth factor; ZEB1, zinc finger E-box binding homeobox 1; SNAI2, snail family transcriptional repressor 2; COL1A1, collagen type Iα1 chain; INHBA, inhibin subunit βA; FN1, fibronectin 1; LUAD, lung adenocarcinoma.

of TGFβ were validated (Fig. S3A-C). It is also important to note that knockdown of YAP (Fig. 4J) significantly attenuated the invasiveness in TD cells, which was similar to the effect identified after *SERPINE1* expression knockdown (Fig. 4K).

Regulation of SEPINE1 expression in the patients with lung adenocarcinoma. To verify the results from the lung cancer cell line model, a transcriptome dataset from 494 patients with lung adenocarcinoma (TCGA; PanCancer Atlas) was obtained from cBioPoral (https//www.cbioportal.org/). *SERPINE1* expression was closely correlated with typical EMT marker genes such as zinc finger E-box binding homeobox 1, *CDH2* and snail family transcriptional repressor 2 (Fig. 5A). Additionally, the YAP-dependent nature of *SERPINE1* expression (Fig. 3) was also supported by the close correlation of *SERPINE1* to CTGF expression (Pearson r=0.5183; Fig. 5B). The TGFβ

dependency of *SERPINE1* expression (Fig. 4) was supported by a close correlation of *SERPINE1* expression to *COL1A1*, inhibin subunit βA (*INHBA*) and fibronectin 1 (*FN1*; Pearson r=0.4267, 0.6200 and 0.4244, respectively), which are typical SMAD4 targets (Fig. 5C). Of note, the CTGF-high patient group demonstrated upregulated expression levels of SMAD4 downstream targets (*COL1A1*, *INHBA* and *FN1*), as well as high *SERPINE1* expression (Fig. 5D), suggesting a crosstalk between TGFβ downstream targets, including *SERPINE1*, and YAP/TAZ gene responses.

From the mRNA expression database involving 566 patients with lung adenocarcinoma, a total of 237 genes were found to be highly correlated with *SERPINE1* expression (Pearson R>0.4), which were then subjected to GO analysis. As predicted, gene signatures of 'ECM matrix organization' (GO: 0030198) and 'cell migration' (GO: 0030334 and 0030335) were highly associated with a *SERPINE1* gene signature in the patients (Fig. 5E; Table SI). Consistent with previous studies (10,43,49), high *SERPINE1* expression was associated with a poor prognosis for relapse or recurrence-free survival but not overall survival (Fig. 5F), indicating that *SERPINE1* expression may have particular relevance to metastasis or recurrence.

Discussion

TGFβ has been extensively characterized as a key stimulus for *SERPINE1* expression and underlies the diverse roles of *SERPINE1* in senescence, fibrosis, vascular disorders and cancer (13,16,50-53). Considering the significant roles of the PA system in controlling ECM remodeling, which itself promotes the invasive and metastatic potential of cancer (5,54), induction of *SERPINE1* in cancer cells is unexpectedly associated with poor prognosis due to its ability to promote metastasis or therapy resistance independent of PA activity(6,10,41,55,56). While the mesenchymal features acquired via EMT (4) have been extensively characterized in both cancer metastasis and therapy resistance, the signaling components responsible for these cancer-promoting mesenchymal features may be important targets for future anti-cancer strategies.

Our previous study observed that *SERPINE1* expression was correlated with chemoresistance score, a common feature of mesenchymal cancer cells (39). Consistent with this finding, the present study identified that *SERPINE1* expression was significantly elevated in TD cells, and was closely correlated with other mesenchymal marker genes in patients with lung cancer. This close correlation with EMT features was recently reported in gastric cancer types via transcriptomic analysis of a large dataset (49). Despite the strong correlation of *SERPINE1* to chemoresistance score, *SERPINE1* knockdown failed to sensitize TD cells to conventional chemotherapeutics (data not shown). Instead, knockdown of *SERPINE1* in TD cells impaired invasive properties in a manner independent of MMP activity. These results were in accordance with data indicating that *SERPINE1* expression served as a more favorable prognostic marker for recurrence-free survival in lung cancer compared with overall survival (Fig. 5F).

The present results suggested that TGFβ-dependent *SERPINE1* expression was distinct between A549 and TD cells. A significant induction of *SERPINE1* expression upon TGFβ treatment was found in TD cells, indicating that a factor(s) activated in TD cells contributed to TGFβ-mediated *SERPINE1* expression, a finding that was similar to previous studies revealing crosstalk among other signaling components underlying the induction of *SERPINE1* expression upon TGFβ stimulation (15,16). The current study demonstrated that YAP, uncontrolled activation of which promotes both development and malignancy in diverse cancer types (57), itself induced *SERPINE1* expression and also contributed to *SERPINE1* expression upon TGFβ treatment. Moreover, a functional interaction between YAP and TGFβ was identified in the regulation of CTGF, which functions as an important growth modulator of malignant mesothelioma (58). The significant reduction of *SERPINE1* expression upon TGFβ by knockdown of YAP suggested that high YAP activity may prime TGFβ-dependent expression. Thus, the significant induction of CTGF by TGFβ in TD cells indicated that the functional interaction between YAP and TGFβ was substantially enhanced in TD cells by an unknown mechanism, which represents as an interesting research question for subsequent studies. It was also observed that immunoblotting for PAI-1 with two commercially available antibodies was technically challenging, unlike that found in previous studies (59,60), for unknown reasons. With multiple attempts, high PAI-1 protein expression in TD cells was barely detected.

In conclusion, the present study demonstrated that *SERPINE1* induction in the mesenchymal lung cancer cells resulted from the synergic effect of YAP and TGFβ, which promoted invasive features. As a cancer prone effect of *SERPINE1* (e.g. invasion) occurs in a PA activity-independent manner, instead of direct inhibitor for *SERPINE1*, a drug(s) to reverse transcriptome signature responsible for *SERPINE1*-dependent invasiveness based on drug-transcripome data analysis (e.g. Connectivity MAP) could be a feasible approach to target the cancer prone effect of *SERPINE1* (39, 61).

Acknowledgements

The authors would like to thank Professor Park Hyun-Woo for providing the YAP expression vectors and GTIIC reporter construct.

Funding

This work was supported by the National Research Foundation of Korea (grant no. NRF-2020R1A2C2005914) and by the Global Core Research Center (grant no. 2011-0030001). This work was also supported by Creative-Pioneering Researchers Program through Seoul National University.

Availability of data and materials

RNA-seq of A549 and TD cell lines can be obtained from Gene Expression Omnibus (GEO) under the accession number GSE135402.

Authors' contributions

HJC conceived the overall study design and led the experiments. HJK and EJK mainly conducted the experiments

and data analysis, as well as provided critical discussion of the results. OSK, HL and WK analyzed clinicogenomics and RNAseq data. JYC and YJK performed the most of genetic perturbation study. All authors contributed to manuscript writing and revising, and approved the final manuscript.

Ethics approval and consent to participate

Not applicable.

Patient consent for publication

Not applicable.

Competing of interests

The authors declare that they have no competing interests.

References

1. Holohan C, Van Schaeybroeck S, Longley DB and Johnston PG: Cancer drug resistance: An evolving paradigm. Nat Rev Cancer 13: 714-726, 2013.
2. Marcucci F, Stassi G and De Maria R: Epithelial-mesenchymal transition: A new target in anticancer drug discovery. Nat Rev Drug Discov 15: 311-325, 2016.
3. Chaffer CL, San Juan BP, Lim E and Weinberg RA: EMT, cell plasticity and metastasis. Cancer Metastasis Rev 35: 645-654, 2016.
4. Shibue T and Weinberg RA: EMT, CSCs, and drug resistance: The mechanistic link and clinical implications. Nat Rev Clin Oncol 14: 611-629, 2017.
5. Andreasen PA, Egelund R and Petersen HH: The plasminogen activation system in tumor growth, invasion, and metastasis. Cell Mol Life Sci 57: 25-40, 2000.
6. Pavón MA, Arroyo-Solera I, Céspedes MV, Casanova I, León X and Mangues R: uPA/uPAR and SERPINE1 in head and neck cancer: Role in tumor resistance, metastasis, prognosis and therapy. Oncotarget 7: 57351-57366, 2016.
7. Pedersen H, Brünner N, Francis D, Osterlind K, Rønne E, Hansen HH, Danø K and Grøndahl-Hansen J: Prognostic impact of urokinase, urokinase receptor, and type 1 plasminogen activator inhibitor in squamous and large cell lung cancer tissue. Cancer Res 54: 4671-4675, 1994.
8. Lin X, Lin BW, Chen XL, Zhang BL, Xiao XJ, Shi JS, Lin JD and Chen X: PAI-1/PIAS3/Stat3/miR-34a forms a positive feedback loop to promote EMT-mediated metastasis through Stat3 signaling in Non-small cell lung cancer. Biochem Biophys Res Commun 493: 1464-1470, 2017.
9. Hirahata M, Osaki M, Kanda Y, Sugimoto Y, Yoshioka Y, Kosaka N, Takeshita F, Fujiwara T, Kawai A, Ito H, *et al*: PAI-1, a target gene of miR-143, regulates invasion and metastasis by upregulating MMP-13 expression of human osteosarcoma. Cancer Med 5: 892-902, 2016.
10. Seker F, Cingoz A, Sur-Erdem İ, Erguder N, Erkent A, Uyulur F, Esai Selvan M, Gümüş ZH, Gönen M, Bayraktar H, *et al*: Identification of SERPINE1 as a regulator of glioblastoma cell dispersal with transcriptome profiling. Cancers (Basel) 11: 11, 2019.
11. Pavón MA, Arroyo-Solera I, Téllez-Gabriel M, León X, Virós D, López M, Gallardo A, Céspedes MV, Casanova I, López-Pousa A, *et al*: Enhanced cell migration and apoptosis resistance may underlie the association between high SERPINE1 expression and poor outcome in head and neck carcinoma patients. Oncotarget 6: 29016-29033, 2015.
12. Kubala MH and DeClerck YA: The plasminogen activator inhibitor-1 paradox in cancer: A mechanistic understanding. Cancer Metastasis Rev 38: 483-492, 2019.
13. Gerwin BI, Keski-Oja J, Seddon M, Lechner JF and Harris CC: TGF-beta 1 modulation of urokinase and PAI-1 expression in human bronchial epithelial cells. Am J Physiol 259: L262-L269, 1990.
14. Kortlever RM, Higgins PJ and Bernards R: Plasminogen activator inhibitor-1 is a critical downstream target of p53 in the induction of replicative senescence. Nat Cell Biol 8: 877-884, 2006.
15. Kawarada Y, Inoue Y, Kawasaki F, Fukuura K, Sato K, Tanaka T, Itoh Y and Hayashi H: TGF-β induces p53/Smads complex formation in the PAI-1 promoter to activate transcription. Sci Rep 6: 35483, 2016.
16. Samarakoon R and Higgins PJ: Integration of non-SMAD and SMAD signaling in TGF-beta1-induced plasminogen activator inhibitor type-1 gene expression in vascular smooth muscle cells. Thromb Haemost 100: 976-983, 2008.
17. Higgins SP, Tang Y, Higgins CE, Mian B, Zhang W, Czekay RP, Samarakoon R, Conti DJ and Higgins PJ: TGF-β1/p53 signaling in renal fibrogenesis. Cell Signal 43: 1-10, 2018.
18. Harvey KF, Zhang X and Thomas DM: The Hippo pathway and human cancer. Nat Rev Cancer 13: 246-257, 2013.
19. Lei QY, Zhang H, Zhao B, Zha ZY, Bai F, Pei XH, Zhao S, Xiong Y and Guan KL: TAZ promotes cell proliferation and epithelial-mesenchymal transition and is inhibited by the hippo pathway. Mol Cell Biol 28: 2426-2436, 2008.
20. Wang Y, Liu J, Ying X, Lin PC and Zhou BP: Twist-mediated epithelial-mesenchymal transition promotes breast tumor cell invasion via inhibition of Hippo pathway. Sci Rep 6: 24606, 2016.
21. Lamar JM, Stern P, Liu H, Schindler JW, Jiang ZG and Hynes RO: The Hippo pathway target, YAP, promotes metastasis through its TEAD-interaction domain. Proc Natl Acad Sci USA 109: E2441-E2450, 2012.
22. Zanconato F, Cordenonsi M and Piccolo S: YAP/TAZ at the roots of cancer. Cancer Cell 29: 783-803, 2016.
23. Dupont S, Morsut L, Aragona M, Enzo E, Giulitti S, Cordenonsi M, Zanconato F, Le Digabel J, Forcato M, Bicciato S, *et al*: Role of YAP/TAZ in mechanotransduction. Nature 474: 179-183, 2011.
24. Sebio A and Lenz HJ: Molecular pathways: Hippo signaling, a critical tumor suppressor. Clin Cancer Res 21: 5002-5007, 2015.
25. Varelas X, Sakuma R, Samavarchi-Tehrani P, Peerani R, Rao BM, Dembowy J, Yaffe MB, Zandstra PW and Wrana JL: TAZ controls Smad nucleocytoplasmic shuttling and regulates human embryonic stem-cell self-renewal. Nat Cell Biol 10: 837-848, 2008.
26. Grannas K, Arngården L, Lönn P, Mazurkiewicz M, Blokzijl A, Zieba A and Söderberg O: Crosstalk between Hippo and TGFβ: subcellular localization of YAP/TAZ/Smad complexes. J Mol Biol 427: 3407-3415, 2015.
27. Szeto SG, Narimatsu M, Lu M, He X, Sidiqi AM, Tolosa MF, Chan L, De Freitas K, Bialik JF, Majumder S, *et al*: YAP/TAZ Are mechanoregulators of TGF-β-Smad signaling and renal fibrogenesis. J Am Soc Nephrol 27: 3117-3128, 2016.
28. Bae GY, Hong SK, Park JR, Kwon OS, Kim KT, Koo J, Oh E and Cha HJ: Chronic TGFβ stimulation promotes the metastatic potential of lung cancer cells by Snail protein stabilization through integrin β3-Akt-GSK3β signaling. Oncotarget 7: 25366-25376, 2016.
29. Livak KJ and Schmittgen TD: Analysis of relative gene expression data using real-time quantitative PCR and the 2(-Delta Delta C(T)) method. Methods 25: 402-408, 2001.
30. Kwon OS, Lee H, Kong HJ, Kwon EJ, Park JE, Lee W, Kang S, Kim M, Kim W and Cha HJ: Connectivity map-based drug repositioning of bortezomib to reverse the metastatic effect of GALNT14 in lung cancer. Oncogene 39: 4567-4580, 2020.
31. Dupont S: Luciferase reporter assays to determine YAP/TAZ activity in mammalian cells. Methods Mol Biol 1893: 121-135, 2019.
32. Vinci M, Box C and Eccles SA: Three-dimensional (3D) tumor spheroid invasion assay. J Vis Exp: May 1, 2015 (Epub ahead of print). doi: 10.3791/52686.
33. Bae GY, Choi SJ, Lee JS, Jo J, Lee J, Kim J and Cha HJ: Loss of E-cadherin activates EGFR-MEK/ERK signaling, which promotes invasion via the ZEB1/MMP2 axis in non-small cell lung cancer. Oncotarget 4: 2512-2522, 2013.
34. Kwon OS, Kwon EJ, Kong HJ, Choi JY, Kim YJ, Lee EW, Kim W, Lee H and Cha HJ: Systematic identification of a nuclear receptor-enriched predictive signature for erastin-induced ferroptosis. Redox Biol 37: 101719, 2020.
35. Love MI, Huber W and Anders S: Moderated estimation of fold change and dispersion for RNA-seq data with DESeq2. Genome Biol 15: 550, 2014.
36. Katsuno Y, Meyer DS, Zhang Z, Shokat KM, Akhurst RJ, Miyazono K and Derynck R: Chronic TGF-β exposure drives stabilized EMT, tumor stemness, and cancer drug resistance with vulnerability to bitopic mTOR inhibition. Sci Signal 12: 12, 2019.
37. Hong SK, Park JR, Kwon OS, Kim KT, Bae GY and Cha HJ: Induction of integrin β3 by sustained ERK activity promotes the invasiveness of TGFβ-induced mesenchymal tumor cells. Cancer Lett 376: 339-346, 2016.

38. Kwon OS, Hong SK, Kwon SJ, Go YH, Oh E and Cha HJ: BCL2 induced by LAMTOR3/MAPK is a druggable target of chemo-radioresistance in mesenchymal lung cancer. Cancer Lett 403: 48-58, 2017.
39. Hong SK, Lee H, Kwon OS, Song NY, Lee HJ, Kang S, Kim JH, Kim M, Kim W and Cha HJ: Large-scale pharmacogenomics based drug discovery for ITGB3 dependent chemoresistance in mesenchymal lung cancer. Mol Cancer 17: 175, 2018.
40. Ghandi M, Huang FW, Jané-Valbuena J, Kryukov GV, Lo CC, McDonald ER III, Barretina J, Gelfand ET, Bielski CM, Li H, *et al*: Next-generation characterization of the Cancer Cell Line Encyclopedia. Nature 569: 503-508, 2019.
41. Klein RM, Bernstein D, Higgins SP, Higgins CE and Higgins PJ: SERPINE1 expression discriminates site-specific metastasis in human melanoma. Exp Dermatol 21: 551-554, 2012.
42. Arroyo-Solera I, Pavón MA, León X, López M, Gallardo A, Céspedes MV, Casanova I, Pallarès V, López-Pousa A, Mangues MA, *et al*: Effect of serpinE1 overexpression on the primary tumor and lymph node, and lung metastases in head and neck squamous cell carcinoma. Head Neck 41: 429-439, 2019.
43. Yang JD, Ma L and Zhu Z: SERPINE1 as a cancer-promoting gene in gastric adenocarcinoma: Facilitates tumour cell proliferation, migration, and invasion by regulating EMT. J Chemother 31: 408-418, 2019.
44. Zhao B, Ye X, Yu J, Li L, Li W, Li S, Yu J, Lin JD, Wang CY, Chinnaiyan AM, *et al*: TEAD mediates YAP-dependent gene induction and growth control. Genes Dev 22: 1962-1971, 2008.
45. Moroishi T, Park HW, Qin B, Chen Q, Meng Z, Plouffe SW, Taniguchi K, Yu FX, Karin M, Pan D, *et al*: A YAP/TAZ-induced feedback mechanism regulates Hippo pathway homeostasis. Genes Dev 29: 1271-1284, 2015.
46. Wada K, Itoga K, Okano T, Yonemura S and Sasaki H: Hippo pathway regulation by cell morphology and stress fibers. Development 138: 3907-3914, 2011.
47. Kutz SM, Hordines J, McKeown-Longo PJ and Higgins PJ: TGF-beta1-induced PAI-1 gene expression requires MEK activity and cell-to-substrate adhesion. J Cell Sci 114: 3905-3914, 2001.
48. Dennler S, Itoh S, Vivien D, ten Dijke P, Huet S and Gauthier JM: Direct binding of Smad3 and Smad4 to critical TGF beta-inducible elements in the promoter of human plasminogen activator inhibitor-type 1 gene. EMBO J 17: 3091-3100, 1998.
49. Xu B, Bai Z, Yin J and Zhang Z: Global transcriptomic analysis identifies SERPINE1 as a prognostic biomarker associated with epithelial-to-mesenchymal transition in gastric cancer. PeerJ 7: e7091, 2019.
50. Hirashima Y, Kobayashi H, Suzuki M, Tanaka Y, Kanayama N and Terao T: Transforming growth factor-beta1 produced by ovarian cancer cell line HRA stimulates attachment and invasion through an up-regulation of plasminogen activator inhibitor type-1 in human peritoneal mesothelial cells. J Biol Chem 278: 26793-26802, 2003.
51. Allan EH, Zeheb R, Gelehrter TD, Heaton JH, Fukumoto S, Yee JA and Martin TJ: Transforming growth factor beta inhibits plasminogen activator (PA) activity and stimulates production of urokinase-type PA, PA inhibitor-1 mRNA, and protein in rat osteoblast-like cells. J Cell Physiol 149: 34-43, 1991.
52. Higgins CE, Tang J, Mian BM, Higgins SP, Gifford CC, Conti DJ, Meldrum KK, Samarakoon R and Higgins PJ: TGF-β1-p53 cooperativity regulates a profibrotic genomic program in the kidney: Molecular mechanisms and clinical implications. FASEB J 33: 10596-10606, 2019.
53. Samarakoon R, Higgins SP, Higgins CE and Higgins PJ: The TGF-β1/p53/PAI-1 signaling axis in vascular senescence: Role of caveolin-1. Biomolecules 9: 9, 2019.
54. Andreasen PA, Kjøller L, Christensen L and Duffy MJ: The urokinase-type plasminogen activator system in cancer metastasis: A review. Int J Cancer 72: 1-22, 1997.
55. Ghosh AK, Rai R, Park KE, Eren M, Miyata T, Wilsbacher LD and Vaughan DE: A small molecule inhibitor of PAI-1 protects against doxorubicin-induced cellular senescence. Oncotarget 7: 72443-72457, 2016.
56. Kang J, Kim W, Kwon T, Youn H, Kim JS and Youn B: Plasminogen activator inhibitor-1 enhances radioresistance and aggressiveness of non-small cell lung cancer cells. Oncotarget 7: 23961-23974, 2016.
57. Moroishi T, Hansen CG and Guan KL: The emerging roles of YAP and TAZ in cancer. Nat Rev Cancer 15: 73-79, 2015.
58. Fujii M, Toyoda T, Nakanishi H, Yatabe Y, Sato A, Matsudaira Y, Ito H, Murakami H, Kondo Y, Kondo E, *et al*: TGF-β synergizes with defects in the Hippo pathway to stimulate human malignant mesothelioma growth. J Exp Med 209: 479-494, 2012.
59. Uchiyama T, Okajima F, Mogi C, Tobo A, Tomono S and Sato K: Alamandine reduces leptin expression through the c-Src/p38 MAP kinase pathway in adipose tissue. PLoS One 12: e0178769, 2017.
60. Li C, Zhu HY, Bai WD, Su LL, Liu JQ, Cai WX, Zhao B, Gao JX, Han SC, Li J, *et al*: MiR-10a and miR-181c regulate collagen type I generation in hypertrophic scars by targeting PAI-1 and uPA. FEBS Lett 589: 380-389, 2015.
61. Kwon OS, Kim W, Cha HJ and Lee H: In silico drug repositioning: From large-scale transcriptome data to therapeutics. Arch Pharm Res 42: 879-889, 2019.